SO4×—based catalytic ceramic UF membrane for organics removal and flux restoration

Suona Zhang, Leonardo Gutierrez, Fei Qi, Jean-Philippe Croué

$SO_4^{\bullet-}$-based catalytic ceramic UF membrane for organics removal and flux restoration

Suona Zhang [a], Leonardo Gutierrez [a,b], Fei Qi [c], Jean-Philippe Croue [a,d]*

[a] Curtin Water Quality Research Centre, Department of Chemistry, Curtin University, Australia

[b] Facultad del Mar y Medio Ambiente, Universidad del Pacifico, Ecuador

[c] College of Environmental Science and Engineering, Beijing Forestry University, Beijing, China

[d] Institut de Chimie des Milieux et des Materiaux IC2MP UMR 7285 CNRS, Universite de Poitiers, France

* Corresponding author: Tel.: +33 (0) 7 87 09 44 66
E-mail address: jean.philippe.croue@univ-poitiers.fr

Abstract

Catalytic membranes have gained increasing interest in water treatment due to their improved performance on contaminants removal, fouling mitigation, and cleaning efficiency. The reactive species generated in the catalytic membrane system play a critical role in the process. However, the performance of $SO_4^{\bullet-}$-based catalytic membrane has been considerably less studied. The current research investigated the performance of a novel $SO_4^{\bullet-}$-based ceramic ultrafiltration membrane on organics removal, fouling mitigation, and cleaning efficiency. The catalytic membrane was prepared through the filtration of a MnO_2-Co_3O_4 nanoparticle solution, followed by sintering and sonication. Characterization results demonstrated the successful deposition of nanoparticles onto the membrane surface. Besides, the influence of 0.06 mg/cm^2 of coating on membrane permeability was negligible. The production of $SO_4^{\bullet-}$ (i.e., with the presence of peroxymonosulfate (PMS)) as predominant radical species was confirmed using *para*-chlorobenzoic acid (*p*CBA) and nitrobenzene (NB) as probe compounds. Due to the reaction with $SO_4^{\bullet-}$, a higher NOM removal rate was observed with the coated membrane as compared to the pristine membrane. However, the permeate flux of the coated membrane was only slightly increased in the presence of PMS (i.e., 8% increase in normalized flux), possibly due to the formation of small molecules leading to internal pore fouling. Contrariwise, the PMS cleaning efficiency with the coated membrane was remarkably higher than the pristine membrane and stable within three cycles of membrane filtration. The results of this study would significantly assist in the optimization of $SO_4^{\bullet-}$-based catalytic membrane processes for future successful industrial implementation.

Keywords: Sulfate radical; Catalytic membrane; Contaminants removal; NOM transformation; Flux restoration.

1. Introduction

Currently, ultrafiltration (UF) is widely implemented as an efficient membrane technology in water treatment [1, 2]. Often used as a pretreatment step, UF exhibits a high capacity for the removal of suspended particles, colloids, and microorganisms [3]. Nevertheless, the removal of small organic pollutants by UF is inefficient [4]. More importantly, the inevitable fouling caused by Natural Organic Matter (i.e., NOM, ubiquitously present in aquatic environments) remains a substantial drawback for this technology. Frequent membrane cleanings are required for restoring the permeate flux caused by fouling. Remarkably, the development of catalytic membranes to address the issue of organic fouling has attracted increasing research interests in recent years.

Catalytic membranes are commonly prepared through surface modification with functionalized materials. Ceramic membranes have nowadays gained increasing interests in both lab-scale research and full-scale water treatment processes due to their stronger thermal, mechanical and chemical properties [5, 6]. Specifically, ceramic membranes are more suitable for the preparation of catalytic membranes due to their stronger chemical stability as compared to their polymeric counterparts. Thus, ceramic membrane filtration integrated with Advanced Oxidation Processes (AOP) generating Reactive Oxygen Species (i.e., ROS, such as $^{\bullet}OH$, $O_2^{\bullet-}$, and $^1O_2$) when used in combination with oxidants or light irradiation is a promising robust technology for tackling organic fouling. Briefly, Byun et al. modified the surface of ceramic membranes with different metal oxides coatings by the layer-by-layer self-assembly technique and observed the highest flux recovery and permeate quality with Mn oxide-coated membrane in combination with ozone treatment [7]. The Mn oxide-coated

membrane was successfully prepared by spreading the metal oxide onto the membrane surface, followed by a sintering process. The modified membrane was demonstrated as capable of mitigating both irreversible and reversible fouling, as well as to enhance the removal of *p*-chloronitrobenzene when coupled with ozone [8]. Besides ozone-based AOPs, photo-Fenton oxidation has also been integrated with a ceramic membrane with catalytic goethite loaded via a cross-linking method. The hybrid process slowed down the fouling kinetics by bovine serum albumin (BSA) and humic acid (HA) with a mineralization rate of over 80% [9].

Catalytic membranes have also shown more efficient flux recovery when using specific oxidants as cleaning agents. For instance, an iron oxide membrane achieved a flux recovery of 97% for HA, 86% for BSA, and 88% for sodium alginate (SA) when H_2O_2 was used as a cleaning reagent [10]. Also, transition metal (i.e., Mn, Cu, Fe, and Co) oxide-coated ceramics showed higher cleaning efficiencies than uncoated ceramic membranes fouled by dyes when peroxymonosulfate (PMS) was used as the cleaning agent [11]. The improved performance in fouling mitigation, permeate quality, and flux recovery was ultimately attributed to the degradation of organics (i.e., NOM and organic pollutants) by ROS generated in the catalytic membrane system. Therefore, ROS-based oxidation processes play a crucial role in the performance of catalytic membranes.

Sulfate radical ($SO_4^{\bullet-}$)-based AOPs have been widely studied as an alternative oxidation technology in the past few years. According to previous studies, this process is capable of degrading a wide variety of organic pollutants due to its high reduction potential [12]. Recently, a MnO_2-integrated ceramic membrane was synthesized and used for degrading

organic pollutants [13]. Up to 98.9% removal of 4-hydroxybenzoic acid was achieved through filtration, mainly relying on $SO_4^{\bullet-}$ generated in the PMS/catalytic membrane. Although fouling mitigation was also observed in that PMS/catalytic membrane system, the transformation or removal of NOM directly linked to fouling was not investigated. Interestingly, $SO_4^{\bullet-}$ has been shown highly efficient in the mineralization of NOM in a Co/PMS system [14]. Therefore, a significant NOM transformation or removal in an $SO_4^{\bullet-}$-based catalytic membrane system would be highly expected; thus, contributing to improved permeate quality, decreased fouling during filtration, and more efficient cleaning processes.

The main goal of this study was to investigate the performance of an $SO_4^{\bullet-}$-based catalytic membrane filtration process. Besides the removal of pollutants, the main focus was also set on NOM transformation, fouling behavior, and cleaning efficiency under various conditions. A novel MnO_2-Co_3O_4 composite was used as a catalytic material for ceramic membrane surface modification, where $SO_4^{\bullet-}$ was generated in the presence of PMS. This Co-based composite catalyst was selected for $SO_4^{\bullet-}$ production because of the reported high catalytic efficiency of Co oxide in PMS decomposition [15]. Also, this hybrid metal oxide has exhibited high efficiency in the activation of ozone into radicals [16]. The catalytic membrane was prepared through the filtration of a MnO_2-Co_3O_4 nanoparticle suspension, followed by sintering and sonication. The $SO_4^{\bullet-}$ production on the catalytic membrane was confirmed by using *p*CBA and NB as a probe compound. Fouling tests were conducted with feedwater prepared with a mixture of well-characterized NOM isolates of different physicochemical properties from various aquatic environments. The change of organics before and after filtration was studied using classic NOM characterization techniques (i.e.,

UV-vis spectrometer, Fluorometer, TOC analyzer). The performance of the modified ceramic membrane towards fouling and cleaning efficiency using PMS solution were also investigated. The results of this study would significantly assist in the optimization of $SO_4^{\bullet-}$-based catalytic membrane processes for future successful industrial implementation.

2. Experimental Section

2.1 Chemicals and materials

HPLC grade Methanol (MeOH, pure) and orthophosphoric acid (H_3PO_4, 85%) were purchased from Honeywell, and hydrochloric acid (HCl, 32%) was supplied by UNIVAR. All the solutions: PMS (Oxone, $2KHSO_5 \cdot KHSO_4 \cdot K_2SO_4$, Sigma-Aldrich), *p*-chlorobenzoic acid (*p*CBA, Acros Organics), nitrobenzene (NB, Sigma-Aldrich), and sodium hydroxide (NaOH, UNIVAR) were prepared with ultrapure water (PURELAB Ultra, ELGA). MnO_2-Co_3O_4 nanoparticles were synthesized through the oxidation of cobaltous nitrate ($Co(NO_3)_2 \cdot 6H_2O$) by potassium permanganate ($KMnO_4$), and then rigorously characterized as previously reported [16]. The ceramic membranes were obtained from TAMI Industries (France), and their characteristics were shown in Table S1, supporting information (SI)

The feedwater was reconstituted using extracted hydrophobic and colloidal NOM isolates: hydrophobic fractions from Suwannee River (HPO-SRNOM, USA) and Blavet River (HPO-Blavet, France) [17], and soluble colloidal fractions from a river in the Brittany Region (Colloids-Brittany, France) [18] and from a nanofiltration (NF) unit (soluble fraction of the biofilm) in the Mery Sur Oise Drinking Water Treatment Plant in Paris (Colloids-Mery, France) (Croué unpublished data). The percentage of colloids in the mixture was approximately 10%; thus, highly representative of natural aquatic environments [19]. The

characteristics of the NOM isolates were detailed in Text S1, SI.

2.2 Preparation and characterization of MnO_2-Co_3O_4 coated ceramic membrane

Prior to use, a sequential cleaning with NaOH, HNO_3, and deionized (DI) water was conducted on the membranes as described elsewhere [20]. Following the cleaning procedures, MnO_2-Co_3O_4-coated ceramic membranes were prepared as follows: MnO_2-Co_3O_4 nanoparticles were dissolved in ultrapure water to obtain a stock nanoparticle suspension of 0.2 g/L. A predetermined amount of the stock nanoparticle solution was diluted in 200 ml of ultrapure water and then filtered through the ceramic membrane at 1 bar. At the end of the filtration, an approximate mass of 0.5–4 mg nanoparticles were loaded onto the ceramic disc with a diameter of 47 mm. Subsequently, the coated membrane was sintered at 550℃ for an hour under air atmosphere and then sonicated for approximately 15 seconds at an operational frequency of 44 kHz. Various analytical techniques were employed for the characterization of the catalytic membrane. To verify the influence of the coating on membrane permeability, the permeate flux of both pristine and coated membranes were recorded with pure water.

2.3 Experimental procedures

Fouling tests were conducted using 100 mL of NOM solution as feedwater in a dead-end mode filtration setup (Fig. S2) at a constant pressure of 1 bar. Instead of buffering the feed solutions, NaOH was used for pH adjustment when needed to avoid the influence of other radical species, such as carbonate/bicarbonate radicals, formed through the oxidation of carbonate/bicarbonate by $SO_4^{\bullet-}$. For the experiments conducted without pH adjustment, no significant pH changes were observed before and after filtration. For feedwater with pH adjusted to ~7.4 by NaOH, the pH slightly changed with no PMS addition. However, the pH dropped by ~2.5 units when

PMS was added in the feedwater. The mass of permeate was recorded using an electronic balance, and the output data were logged through a data acquisition system. The change in permeate flux was calculated based on the collected data. Specifically, permeate flux (J, L m^{-2} h^{-1}) was obtained from equation (1):

$$J = \frac{V}{At} \quad (1)$$

Where V (L) is the volume of permeate, A (m^2) is the effective membrane area, and t (h) is the filtration time. Flux decline (F_d, %) was calculated as

$$F_d(\%) = (1 - \frac{J}{J_0}) \times 100 \quad (2)$$

Where J (L m^{-2} h^{-1}) and J_0 (L m^{-2} h^{-1}) are the permeate fluxes at the end and the beginning of each filtration cycle. Retention rate (R, %) of organic foulants was calculated from:

$$R(\%) = (1 - \frac{C_p}{C_0}) \times 100 \quad (3)$$

Where C_p is the UV_{254} or TOC in the 100 mL of permeate, and C_0 is the initial UV_{254} or TOC in the feedwater. Different cleaning methods were used for the flux restoration of the fouled membrane. Backwash was conducted by flushing the inverted fouled ceramic in the membrane cell with an operational pressure of 1.25 Bar. Chemical cleaning was performed by either filtering 100 ml of 10 mM PMS solution through the fouled membrane or by soaking fouled ceramic membranes in 10 mM HCl, NaOH, or PMS solution at room temperature (20 ± 1 ℃).

The average permeate flux of the cleaned membrane with pure water was expressed as J_c (L m^{-2} h^{-1}). The flux recovery rate was calculated as:

$$Fr(\%) = \left(\frac{Jc}{J_0}\right) \times 100 \quad (4)$$

Membrane resistance (Rs, m^{-1}) was calculated based on the following equation:

$$Rs(m^{-1}) = \frac{\Delta P}{\mu J} \quad (5)$$

Where ΔP is the operational pressure (Pa), μ is the dynamic viscosity (Pa • s) of the NOM solution, and J is the permeate flux (L m^{-2} h^{-1}).

2.4 Analytical methods

The hydrodynamic diameter and Zeta potential of MnO_2-Co_3O_4 nanoparticles were measured with a Zetasizer (Nano ZS, Malvern, UK) as previously described [21]. The catalytic behavior of the nanoparticles was studied by calculating the rate of PMS decomposition, where the PMS residual was measured using a method described in a previous study [14]. The oxidation state of each element on the membrane was characterized by X-ray photoelectron spectroscopy (XPS, PerkinElmer, USA), and the topography was studied using atomic force microscopy (AFM, Bruker, USA).

The change in *p*CBA and NB (both at an initial concentration of 2 μM) under 1 min interval filtration was studied with an HPLC unit equipped with a 250 mm × 4.6 mm C18 5-μm reverse phase column (AlltimaTM, GRACE) and UV detector (Agilent 1100 series, USA). The mobile phase was composed of 60% MeOH and 40% pure water (0.1% H_3PO_4), while

the flowrate was set to 1mLmin^{-1}. The concentration of the probe compounds after filtration was presented as an average of the multiple results within 5 min. The detecting wavelength was set to 238 nm and 270 mm for *p*CBA and NB, respectively. The UV light absorbance at 254 nm (UV_{254}) of different solutions was analyzed using a Cary 60 spectrophotometer (Agilent, USA). The total organic carbon content in the feedwater and permeate was measured with a Shimadzu TOC-L analyzer (SHIDMAZU, Japan). Fluorescence excitation and emission matrices (EEM) were acquired with a Fluorescence spectrometer (Cary Eclipse, Varian) based on the method from Chen et al. [22]. The metal leaching content was analyzed using an inductively coupled plasma mass spectrometry (ICP-MS, Agilent Technology) with a detection limit of 0.0001mg/L.

3. Results and Discussion

3.1. Characterization MnO_2-Co_3O_4 coated catalytic membrane

MnO_2-Co_3O_4 nanoparticles were successfully dispersed onto the membrane surface through filtration of nanoparticles suspension, as indicated by the optical images of the pristine and coated ceramics (Fig. S3a). The observation could also be supported by the measurement of a larger hydrodynamic diameter (~136 nm) of the nanoparticles than the pore size (~8.6 nm) of the pristine membrane (Text S2, SI). Sonication was applied to remove loosely-bound nanoparticles. Remarkably, following sonication of 15 sec (i.e., at an operational frequency of 40 kHz), the dispersed nanoparticles mostly remained stable on the surface. The elemental composition of the nanoparticles was also investigated through XPS analysis (Text S3, Fig. S5).

Atomic Force Microscopy (AFM) was used to investigate the topography and chemical mapping (i.e., phase imaging) of the surface of the membranes. Briefly, the surface of both membranes was physically heterogeneous at the nano-scale (Fig. S3b). However, the MnO_2-Co_3O_4 coating slightly decreased the surface roughness as indicated by its lower roughness (R_{RMS}: 45.1 ± 5.9 versus 50.9 ± 5.5 nm). This lower roughness would be caused by the entrapment of nanoparticles in the valleys on the membrane surface; thus, increasing the stability of the nanoparticles on the membrane surface. Phase images (i.e., chemical mapping of surfaces based on the differences in elemental composition) showed the difference in the elemental composition of pristine and coated membranes; thus, indicating successful adsorption of the nanoparticles on the ceramic membranes (Fig. S3c). Moreover, the occurrence of different oxidation states of Mn (i.e., Mn(IV) and Mn(III)) and Co (i.e., Co(III) and Co(II)) was confirmed through XPS analysis (Text S3). The permeability with pure water was also measured and compared between pristine and coated membranes. The incorporation of 1 mg MnO_2-Co_3O_4 nanoparticles showed a minor effect on the permeability of membranes (i.e., 370.5 $Lm^{-2}h^{-1}bar^{-1}$ and 340.33 $Lm^{-2}h^{-1}bar^{-1}$ for pristine and coated membranes, respectively) (Fig. S6).

Fig. 1

With the filtration of pure water, a coating of 0.5–4.0 mg catalyst showed a minor influence on the pure water flux or intrinsic membrane resistance (i.e., < 10%, Table S2) as compared to the pristine membrane. The water flux and TOC retention rate for both pristine and coated membranes were also measured with the filtration of NOM (~5 mgC/L) solutions. The NOM solution was a mixture of previously isolated colloidal (~10%) and hydrophobic fractions (~90%) selected based on their fouling behaviors (Text S4, SI) and environmental relevance.

Following the filtration of 100 mL NOM solution, a 40% decrease in water flux (Fig. 1), a 67% increase in membrane resistance (Table S2) and a 30% NOM retention rate (Fig. 1) were recorded with the pristine membrane. With the incorporation of MnO_2-Co_3O_4 nanoparticles, a decrease in water flux (Fig. 1a, and profiles of original flux were present in Fig. S7) and an increase in membrane resistance (Table S2) as well as NOM retention rate (Fig. 1b) were observed. Moreover, an increase in the nanoparticle loadings led to a more pronounced change in these parameters. For instance, a coating of 0.5 mg nanoparticles only led to a 48% decrease in water flux, a 94% increase in membrane resistance, and a 38% NOM retention rate. However, a 65% decrease in water flux, a 185% increase in membrane resistance, and a 56% NOM retention rate were achieved with a 4 mg MnO_2-Co_3O_4 nanoparticle coating. The results clearly indicate that increasing nanoparticle load could induce an additional decrease in water flux and an increase in membrane resistance as well as NOM retention rate. To minimize the influence of the coating on water flux and maximize the catalytic ability, a coating of 1mg MnO_2-Co_3O_4 nanoparticles (i.e., 0.06 mg/cm^2) was selected for the following experimental conditions and analysis.

3.2 Catalytic performance of the coated membrane

Fig. 2

The generation of reactive species was confirmed through the filtration of probe compound-containing solution in the presence of 1mM PMS. The removal efficiency of *p*CBA and NB (i.e., used as $SO_4^{\bullet-}$ and $^{\bullet}OH$ probe compounds, respectively) under different experimental conditions were shown in Fig. 2. The removal of *p*CBA by sole PMS or adsorption was negligible under both pH conditions (i.e., pH 3.40 and 7.40), while approximately 20% adsorption efficiency was observed with NB. The adsorption of NB onto

MnO_x- or TiO_2- based catalyst has also been reported in previous studies [23, 24]. Upon addition of PMS (i.e., probe compound-containing solution), a significant increase in *p*CBA removal was observed with the coated membrane as compared to the pristine membrane (Fig. 2a). In addition, the removal efficiency was enhanced with an increase in pH. The removal rate increased from 35% at pH 3.40 to 70% at pH 7.40. This improved catalytic performance was probably caused by an enhancement in radical production and/or the increase in the reactivity of *p*CBA at higher pH conditions [25]. Specifically, the deprotonated form of *p*CBA at a pH significantly higher than its pKa (i.e., 3.98) is more reactive to radicals. The removal of NB through the hybrid PMS-catalytic membrane process was insignificant at pH 3.40; however, this removal increased to 54% with a pH adjusted to 7.40. The increase in NB removal at higher pH could probably be attributed to the favorable conversion of OH^- to $^{\bullet}OH$ under caustic conditions. Overall, these findings suggested that reactive species were generated through the catalytic decomposition of PMS by the MnO_2-Co_3O_4 nanoparticles coated on the membrane. In addition, the higher removal of *p*CBA than NB indicated the predominance of $SO_4^{\bullet-}$ in the catalytic membrane system. The results also implied that organic pollutants susceptible to these radical species could be potentially removed by the catalytic membrane.

3.3 Fouling behavior of catalytic membrane

3.3.1 Transformation of organic foulants

Fig. 3

The change in UV_{254} of the NOM solution (i.e., mixture of Colloids and HPO-SRNOM) following membrane filtration was investigated as aromaticity has been reported to play an important role in membrane fouling [26]. The varying trend of UV_{254} values of the NOM

solutions before and after filtration was measured for both pristine and coated membranes under varying conditions. The initial UV_{254} value for both NOM solutions was similar at approximately 0.18 (cm^{-1}). The absorbance was predominantly contributed by the HPO fractions due to the negligible UV absorbance of the colloidal fractions (i.e., SUVA <0.4 $m^{-1}(mgC/L)^{-1}$). Under sole membrane filtration (red bar in Fig. 3a), a decrease in UV_{254} value in the permeate was observed for both pristine and coated membranes. The difference in the UV_{254} retention rate between pristine and coated membranes was insignificant. Interestingly, a higher removal in UV_{254} was recorded for NOM solution-M (i.e., 0.55 mgC/L Colloids-Mery + 4.45 mgC/L HPO-SRNOM) than for NOM solution-B (0.56 mgC/L Colloids-Brittany + 4.45 mgC/L HPO-SRNOM) i.e., 50% and 40%, respectively. As Colloids-Mery showed higher fouling potential than Colloids-Brittany (Text S4, SI), the higher UV_{254} removal for NOM solution-M than solution-B could be caused by the increased retention of HPO fractions due to enhanced interactions with Colloids-Mery. With the addition of 1mM PMS in the feedwater, the UV_{254} removal efficiency was further increased (green bar in Fig. 3a). This increase was higher for coated membrane than pristine membrane; specifically, 20.7% versus 6.2% for NOM solution-B, and 17.1% versus 2.6% for NOM solution-M, respectively. This could be attributed to the enhanced reaction between NOM and $SO_4^{\bullet-}$ generated in the catalytic membrane system. The slightly enhanced UV_{254} removal with the pristine membrane was probably due to the reaction of electron-rich moieties with PMS [11], as its production of radical species was detected as negligible (Fig. 2).

The TOC removal rate of the two NOM solutions through either sole membrane filtration or hybrid oxidation-filtration process was also measured. Consistent with the trend observed

with the UV_{254} retention rate, the TOC retention rate (red bar in Fig. 3b) was higher for NOM solution-M than NOM solution-B under sole membrane filtration. Consistently, the difference in the change of specific UV absorbance at 254 nm (i.e., SUVA) value before and after filtration was insignificant between NOM solution-M and NOM solution-B (Table S3). However, the difference in TOC retention rate between NOM solution-M and NOM solution-B was higher than that of UV_{254}. This could also be explained by the distinct fouling potential of the two colloidal fractions in each NOM solution. Not only the moieties with larger molecular size (colloids and high MW UV light-absorbing structures) could be easily withheld, the relatively smaller molecular weight moieties (i.e., less enriched in aromatic structures) could also be screened out due to a probably more efficient interaction of HPO molecules with Colloids-Mery. Similarly, the TOC removal efficiency was significantly increased during the hybrid oxidation-filtration process, i.e., 16.9% versus 4.8% for NOM solution-B, and 14.1% versus 2.0% for NOM solution-M. Moreover, the removal rate of SUVA was also higher with PMS/coated membrane than PMS/pristine membrane process (i.e., 29% versus 16%, Table S3), indicating a more efficient removal of aromatic structures of the former. Overall, the enhanced removal of aromatics, as well as TOC, would be attributed to the transformation or removal of the organic foulants through reaction with the generated $SO_4^{\bullet-}$ and leading to a more NOM-reduced permeate.

Although an increased removal efficiency for *p*CBA and NB was observed at pH 7.40, the change in the removal efficiency of UV_{254} and TOC was negligible when pH was increased to 7.40 (i.e., within 7%, Fig. S9). This could be ascribed to the highly heterogeneous nature of NOM as compared to simple compounds. Specifically, the change in reactivity with pH

would not be as significant as a simple compound (i.e., *p*CBA, Fig.2). The results indicated that the performance of the catalytic membrane would be stable at a pH range from 3.40–7.40, and the catalytic membrane would also be applicable in multiple aquatic environments (e.g., natural water, wastewater, etc). These results also confirmed that the increase in UV_{254} or TOC removal rate with PMS addition was a product of radical production instead of pH change.

3.3.2 Change of fouling profile

Fig. 4

The water flux of the pristine and coated membrane with or without PMS addition in NOM solution-B or NOM solution-M were also studied at unadjusted pH. As shown in Fig. 4 (i.e., results selected as representative of multiple tests showing the same trend), an approximately 50% flux decline was measured for both membranes upon filtration of 100 mL NOM solution-B or NOM solution-M. With the addition of 1mM PMS, the flux increase was only 8% for the coated membrane, slightly higher than the pristine membrane (i.e., 4%). Moreover, the influence of pH on fouling mitigation was negligible (Fig. S10, fouling profile obtained at pH 7.40). Despite a higher removal in UV_{254} or TOC in the PMS/coated membrane process, the improvement in fouling mitigation was insignificant possibly due to the formation of lower molecular weight organics (i.e., as reflected by the blue shift of the peaks in fluorescence spectra, Text S5) adsorbing onto the internal wall of the membrane pores and consequently causing more fouling through pore constriction. Specifically, the fouling could be caused by the interaction of treated NOM molecules with the membrane through hydrogen-bonding due to the formation of hydroxylated products with $SO_4^{\bullet-}$ oxidation [14].

The fouling mitigation effect of catalytic membranes has been less investigated as compared to its performance on organic pollutant removal [8, 16]. Interestingly, an insignificant flux increase (i.e., approximately 10%) has also been observed with an Mn oxide integrated catalytic ceramic membrane [13]. However, the possible reasons causing this minor effect were not provided. To explain the observations in the current study, fouling mechanisms under varying conditions were investigated using filtration models. Membrane fouling can be classified into four categories: Complete pore blocking, intermediate pore blocking, standard pore constriction, and cake layer filtration [27]. The equations and descriptions for different filtration models were listed in Table S4. The R^2 values obtained from the fitting of the experimental data using the fouling model equations were summarized in Table 1. As reflected by the R^2 values in Table 1, the standard blocking model displayed the best fitting to the experimental data under all experimental conditions, where an R^2 value of up to 1.000 was calculated. These results indicated the predominance of pore constriction caused by the deposition of foulants onto the internal wall of the membrane pores. Nevertheless, other fouling mechanisms may also play a role in fouling evolution (Table 1). The reaction with $SO_4^{\bullet-}$ would more likely occur for organics adsorbed at the membrane surface where the MnO_2-Co_3O_4 nanoparticles would mainly be present (section 3.1), and radical species were generated. Consequently, the oxidation of the organics trapped within membrane pores might not be efficient, probably due to its short-lived nature or unfavorable radical diffusion (e.g., quenching by NOM molecules in liquid phase). Consequently, the overall percentage of the organics exposed to radical would be small because the majority of the organics would deposit on the internal wall of the membrane pore channel as revealed by the predominant

fouling mechanism. Specifically, only larger molecules, i.e., Colloids-HPO complex could react with radicals due to their higher possibility of deposition onto the membrane surface. However, the increased fouling caused by the formation of smaller molecules and their subsequent adsorption on the pore channel could not be reflected by these fitting results, as a fouling mechanism of standard pore constriction was already predominant during sole filtration (i.e., absence of PMS in NOM solution, Table 1).

Table 1

3.4 Cleaning efficiency of catalytic membrane

Fig. 5

The performance of PMS cleaning for both the pristine and coated membrane was studied through flux restoration. PMS cleaning was conducted by the filtration of 10 mM PMS solution through the fouled membrane at pH 3.20. As shown in Fig. 5 (i.e., representative results of multiple cleaning tests), a higher flux recovery was obtained with the coated membrane for both NOM solutions. In addition, the flux recovery was faster at the beginning of the cleaning phase and then slowed down. Specifically, the flux was recovered from 46% to 82% for NOM solution-B and from 50% to 62% for NOM solution-M with the filtration of 50 mL of PMS solution. However, the flux was only increased by approximately 5% with another 50 mL PMS solution. This low flux recovery was probably due to a faster reaction of HPO fractions (i.e., major fraction of NOM solution) with $SO_4^{\bullet-}$ at the initial phase, as previously reported [14]. Moreover, PMS cleaning for the NOM solution-B fouled membrane was more efficient as compared to that fouled by NOM solution-M. Prolonged cleaning time was applied to further improve the cleaning efficiency as the increase in flux slowed down

during the cleaning. As an alternative, PMS cleaning was conducted by soaking the fouled membrane in 10 mM PMS solution for different time durations. The results for the membrane fouled by NOM solution-M (i.e., selected as a representative experimental result) showed a slower flux restoration. After a soaking time of 10 min, equivalent to the time frame for filtering 100 mL of 10 mM PMS solution through the membrane, the water flux was recovered by 19 ± 0.1% (Fig. S12), which was higher than that of the former cleaning method (i.e., 12%). The observation seems to indicate that the reaction of NOM with radicals was more favorable under static conditions.

Full flux recovery was achieved when the soaking time was prolonged to 2 hours, which equals to a flux increase of approximately 50% (Fig. 6a). The efficiency of other cleaning methods, i.e., backwashing, HCl, and NaOH cleaning, was also investigated. As it was shown in Fig. 6a, PMS cleaning exhibited a significant increase in water flux as compared to other cleaning means. In addition, the flux recovery by PMS cleaning for the pristine membrane was lower than the coated membrane (i.e., 75% versus 97%). The increase in water flux for the pristine membrane could be attributed to the reaction of NOM with PMS [11]. However, the significantly improved cleaning efficiency for the coated membrane would be attributed to the catalytic process, where reactive radical species (i.e., mainly $SO_4^{\bullet-}$) were produced through MnO_2-Co_3O_4 nanoparticles-catalyzed PMS decomposition. The organic foulants could be transformed/degraded and removed by the generated $SO_4^{\bullet-}$ with sufficient exposure time, leading to the observed cleaning performance of the coated membrane.

The applicability of PMS cleaning was further evaluated by performing different fouling cycles with both pristine and coated membranes. The filtration of 100 mL NOM solution-M

(pH 6.28) followed by PMS cleaning with a soaking time of 2 hours were included in each cycle. The normalized water flux decreased to approximately 55% at the end of fouling test (cycle 1) (Fig. 6b). Following PMS cleaning, a full flux recovery was observed with the coated membrane, and a flux recovery of 82% was recorded with the pristine membrane, leading to a lower initial flux at the beginning of the second filtration cycle. The flux recovery was negligible with PMS cleaning for the pristine membrane at cycle 2; however, the normalized flux increased to 80% for the coated membrane. These results indicated that the catalytic membrane not only exhibited better performance with PMS cleaning but also remained relatively stable in performance within 3 cycles of filtration.

Fig. 6

3.5 Metal leaching

The content of leached metals in permeate, i.e., Mn and Co, from MnO_2–Co_3O_4 nanoparticles was measured under different experimental conditions (Table S5). The leaching level was higher at acidic conditionos (i.e., pH 3.40) than in basic environments (i.e., pH 7.40). Besides, metal leaching increased after the first cycle of PMS cleaning and decreased after the second cycle of PMS cleaning. Overall, the concentration of leached Mn ranged from 0.002–0.04 mg/L, accounting for 0.2%–3.7% of MnO_2-Co_3O_4 nanoparticles coated on the membrane (1 mg). The concentration of leached Co was measured as 0.008–0.1 mg/L, accounting for 1.4%–10% of the weight of the coated catalyst. The concentration of leached Mn in the current experiments falls within the range of Mn detected in freshwaters, 0.001–0.2 mg/L [28]. Leached Co level is higher than that reported for surface water or groundwater ranging from

<1μg/L to 1–10μg/L[29], suggesting the need for developing efficient Co-based catalyst with less metal leaching.

4. Conclusions and Future Perspectives

MnO_2-Co_3O_4 coated ceramic UF membrane was prepared through a membrane filtration of nanoparticle suspensions followed by sintering and sonication. The incorporation of 1 mg nanoparticles (i.e., 0.06 mg/cm^2) onto the membrane slightly decreased the surface roughness and showed an insignificant impact on the membrane permeability with pure water. The catalytic property of the MnO_2-Co_3O_4 coated membrane was confirmed with the remarkable removal of *p*CBA during the hybrid oxidation and filtration process. $SO_4^{\bullet-}$ was found as the predominant radical species in the catalytic membrane system because of the higher removal efficiency of *p*CBA than NB. Compared with the pristine membrane, the coated membrane showed a more robust removal of organic foulants with PMS added in the feedwater as well as a higher cleaning efficiency with PMS as a cleaning agent. However, the improvement in permeate flux during fouling tests with PMS added in feedwater was insignificant, probably due to the unfavorable radical oxidation of the organic molecules adsorbed onto the internal walls of membrane pores under the current experimental conditions. The current study provided a comprehensive insight into the performance of the $SO_4^{\bullet-}$-based catalytic membrane process.

Further studies are highly required to improve the performance of the catalytic membrane on fouling control. A coating on the membrane surface, as well as onto the inner walls of membrane pores, could be developed to increase the efficiency of radical production.

Alternatively, to avoid the additional loss of permeability due to catalyst introduction, lab-scale manufacture of membranes with catalytic materials as the working layer could be considered for dynamic radical production. In addition, the development of highly efficient catalysts with lower or no metal leaching is beneficial and required for the successful implementation of the $SO_4^{\bullet-}$-based catalytic membrane process in the industry.

Acknowledgements

The authors acknowledge the China Scholarship Council and Curtin University for providing the PhD scholarship to Suona Zhang. Dr. Franca Jones, Dr. Mark Hackett, Shaghraf Javaid, and Wei Chen in the School of Molecular and Life Sciences at Curtin University are also acknowledged for their valuable help in XPS data analysis.

Appendix A. Supporting Information

Supporting information associated with this article can be found, in the online version, at http://

References

1. Wolf, P.H., S. Siverns, and S. Monti, *UF membranes for RO desalination pretreatment.* Desalination, 2005. **182**(1): p. 293-300.
2. Gao, W., et al., *Membrane fouling control in ultrafiltration technology for drinking water production: A review.* Desalination, 2011. **272**(1): p. 1-8.
3. Winter, J., W. Uhl, and P.R. Bérubé, *Integrated oxidation membrane filtration process – NOM rejection and membrane fouling.* Water Research, 2016. **104**: p. 418-424.
4. Yoon, Y., et al., *Nanofiltration and ultrafiltration of endocrine disrupting compounds, pharmaceuticals and personal care products.* Journal of Membrane Science, 2006. **270**(1): p. 88-100.
5. Kim, J., et al., *Effect of ozone dosage and hydrodynamic conditions on the permeate flux in a hybrid ozonation–ceramic ultrafiltration system treating natural waters.* Journal of Membrane Science, 2008. **311**(1): p. 165-172.
6. Lehman, S.G. and L. Liu, *Application of ceramic membranes with pre-ozonation for treatment of secondary wastewater effluent.* Water Research, 2009. **43**(7): p. 2020-2028.
7. Byun, S., et al., *Mn oxide coated catalytic membranes for a hybrid ozonation–membrane filtration: Comparison of Ti, Fe and Mn oxide coated membranes for water quality.* Water Research, 2011. **45**(1): p. 163-170.
8. Cheng, X., et al., *Fabrication of Mn oxide incorporated ceramic membranes for membrane fouling control and enhanced catalytic ozonation of p-chloronitrobenzene.* Chemical Engineering Journal, 2017. **308**: p. 1010-1020.
9. Sun, S., et al., *Reactive Photo-Fenton ceramic membranes: Synthesis, characterization and antifouling performance.* Water Research, 2018. **144**: p. 690-698.
10. De Angelis, L. and M.M.F. de Cortalezzi, *Improved membrane flux recovery by Fenton-type reactions.* Journal of Membrane Science, 2016. **500**: p. 255-264.
11. Zhao, Q., et al., *Peroxymonosulfate-based cleaning technology for metal oxide-coated ceramic ultrafiltration membrane polluted by Alcian Blue 8GX dye: Radical and non-radical oxidation cleaning mechanism.* Journal of Membrane Science, 2019. **573**: p. 210-217.
12. Lutze, H.V., N. Kerlin, and T.C. Schmidt, *Sulfate radical-based water treatment in presence of chloride: Formation of chlorate, inter-conversion of sulfate radicals into hydroxyl radicals and influence of bicarbonate.* Water Research, 2015. **72**: p. 349-360.
13. Wu, H., et al., *Manganese oxide integrated catalytic ceramic membrane for degradation of organic pollutants using sulfate radicals.* Water Research, 2019. **167**: p. 115110.
14. Zhang, S., et al., *Reactivity of chromophoric dissolved organic matter (CDOM) to sulfate radicals: Reaction kinetics and structural transformation.* Water Research, 2019. **163**: p. 114846.
15. Anipsitakis, G.P., E. Stathatos, and D.D. Dionysiou, *Heterogeneous activation of Oxone using Co 3O 4.* Journal of Physical Chemistry B, 2005. **109**(27): p. 13052-13055.
16. Guo, Y., B. Xu, and F. Qi, *A novel ceramic membrane coated with MnO2–Co3O4 nanoparticles catalytic ozonation for benzophenone-3 degradation in aqueous solution: Fabrication, characterization and performance.* Chemical Engineering Journal, 2016. **287**: p. 381-389.
17. Croue, J.-P., G.V. Korshin, and M.M. Benjamin, *Characterization of natural organic matter in drinking water*. 2000: American Water Works Association.

18. Lee, N., G. Amy, and J.-P. Croué, *Low-pressure membrane (MF/UF) fouling associated with allochthonous versus autochthonous natural organic matter.* Water Research, 2006. **40**(12): p. 2357-2368.
19. Wershaw, R.L., J.A. Leenheer, and L.G. Cox, *Characterization of dissolved and particulate natural organic matter (NOM) in Neversink Reservoir, New York*. 2005.
20. Lu, D., et al., *Hydrophilic Fe2O3 dynamic membrane mitigating fouling of support ceramic membrane in ultrafiltration of oil/water emulsion.* Separation and Purification Technology, 2016. **165**: p. 1-9.
21. Zhang, S., et al., *The characteristics of organic matter influence its interfacial interactions with MnO2 and catalytic oxidation processes.* Chemosphere, 2018. **209**: p. 950-959.
22. Chen, W., et al., *Fluorescence Excitation−Emission Matrix Regional Integration to Quantify Spectra for Dissolved Organic Matter.* Environmental Science & Technology, 2003. **37**(24): p. 5701-5710.
23. Yang, Y., et al., *Degradation of nitrobenzene by nano-TiO2 catalyzed ozonation.* Journal of Molecular Catalysis A: Chemical, 2007. **267**(1): p. 41-48.
24. Ma, J., et al., *Effect of pH on MnOx/GAC catalyzed ozonation for degradation of nitrobenzene.* Water Research, 2005. **39**(5): p. 779-786.
25. Benner, J. and T.A. Ternes, *Ozonation of Metoprolol: Elucidation of Oxidation Pathways and Major Oxidation Products.* Environmental Science & Technology, 2009. **43**(14): p. 5472-5480.
26. Aoustin, E., et al., *Ultrafiltration of natural organic matter.* Separation and Purification Technology, 2001. **22-23**: p. 63-78.
27. Shen, Y., et al., *A systematic insight into fouling propensity of soluble microbial products in membrane bioreactors based on hydrophobic interaction and size exclusion.* Journal of Membrane Science, 2010. **346**(1): p. 187-193.
28. WHO, *Manganese in drinking-water: Background document for development of WHO Guidelines for Drinking-water Quality*. 2004, World Health Organization.
29. Kim, J.H., H.J. Gibb, and P.D. Howe, *Cobalt and inorganic cobalt compounds*. 2006: World Health Organization.

Figure captions

Fig. 1. (a) Normalized flux decline, and (b) TOC retention rate for coated membranes with different MnO_2-Co_3O_4 loadings (0.0–4.0 mg). Fouling experiments were conducted with NOM-containing feedwater (~5 mgC/L NOM mixture with ~10% colloids and ~90% HPO fractions) at unadjusted pH of 6.3 ± 0.2 and operating pressure of 1bar.

Fig. 2. (a) *p*CBA and (b) NB removal during filtration with pristine and coated membranes with or without PMS addition. Conditions: $[pCBA]_0$ = 2 µM, $[NB]_0$ = 2 µM, $[PMS]_0$ = 1 mM, TMP = 1.0 bar, temperature = 20 ± 1°C, pH = 5.20 ± 0.20 without PMS addition and 3.40 ± 0.10 with PMS addition without pH adjustment, pH was adjusted to 7.40 ± 0.20 with 0.01M NaOH for both sole and catalytic filtration process.

Fig. 3. (a) UV_{254} and (b) TOC removal rate with pristine and coated membranes. NOM solution-B: 0.56 mgC/L Colloids-Brittany + 4.45 mgC/L HPO-SRNOM, and NOM solution-M: 0.55mgC/L Colloids-Mery + 4.45 mgC/L HPO-SRNOM. Experimental conditions: Operational pressure =1.0 bar, temperature 20 ± 1°C, pH ~ 6 without PMS addition and 3.40 ± 0.10 with 1 mM PMS addition.

Fig. 4. Normalized water flux of the pristine and coated membrane with or without PMS addition in (a) NOM solution-B and (b) NOM solution-M. NOM solution-B: 0.56 mgC/L Colloids-Brittany + 4.45 mgC/L HPO-SRNOM, NOM solution-M: 0.55 mgC/L Colloids-Mery + 4.45 mgC/ L HPO-SRNOM. Experimental conditions: Operational pressure =1.0 bar, temperature 20 ± 1 °C, pH ~ 6 without PMS addition, and 3.40 ± 0.10 with 1 mM PMS addition.

Fig. 5. Change in normalized water flux during fouling test and PMS cleaning for (a) NOM solution-B and (b) NOM solution-M fouled membrane. Conditions: Fouling tests were conducted with 100 mL of feedwater containing 0.56 mgC/L Colloids-Brittany + 4.45 mgC/L HPO-SRNOM for (a) and 0.55 mgC/L Colloids-Mery + 4.45 mgC/ L HPO-SRNOM for (b). Cleaning was performed with 100 mL of 10 mM PMS solution at pH 3.20 ± 0.10.

Fig. 6. Flux recovery rate with (a) multiple cleaning methods and (b) fouling profiles during filtration cycles with PMS cleaning applied between each fouling cycle for both pristine and coated membranes. Feedwater for fouling tests was prepared with a mixture of 0.55 mgC/L Colloids-Mery and 4.45 mgC/L HPO-SRNOM (pH 6.28). The black dash lines in Fig. 7a indicate the range of the values in normalized water flux before cleaning.

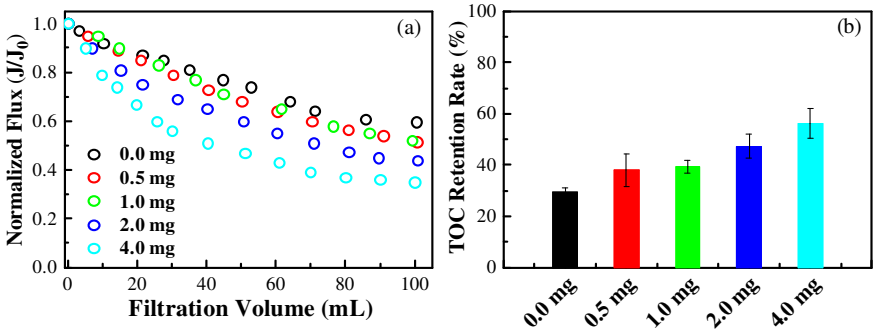

Fig. 1. (a) Normalized flux decline, and (b) TOC retention rate for coated membranes with different MnO_2-Co_3O_4 loadings (0.0–4.0 mg). Fouling experiments were conducted with NOM-containing feed water (~5 mgC/L NOM mixture with ~10% colloids and ~90% HPO fractions) at unadjusted pH of 6.3 ± 0.2 and operating pressure of 1bar.

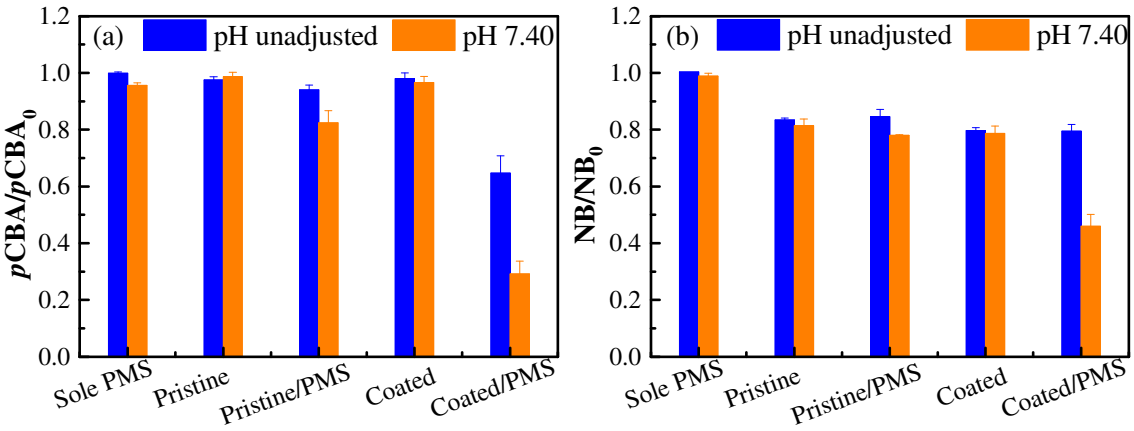

Fig. 2. (a) *p*CBA and (b) NB removal during filtration with pristine and coated membranes with or without PMS addition. Conditions: $[pCBA]_0 = 2$ µM, $[NB]_0 = 2$ µM, $[PMS]_0 = 1$ mM, TMP = 1.0 bar, temperature = 20 ± 1°C, pH = 5.20 ± 0.20 without PMS addition and 3.40 ± 0.10 with PMS addition without pH adjustment, pH was adjusted to 7.40 ± 0.20 with 0.01M NaOH for both sole and catalytic filtration process.

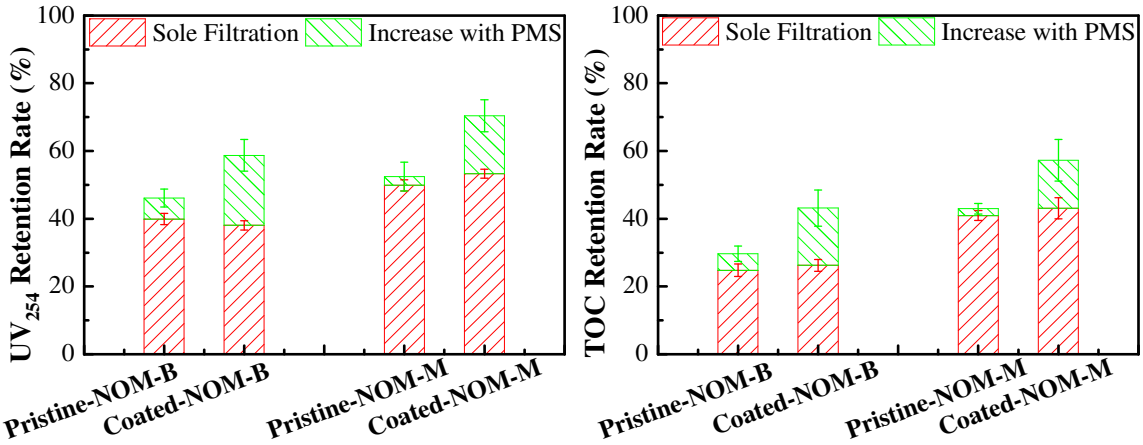

Fig. 3. (a) UV_{254} and (b) TOC removal rate with pristine and coated membranes. NOM solution-B: 0.56 mgC/L Colloids-Brittany + 4.45 mgC/L HPO-SRNOM, and NOM solution-M: 0.55mgC/L Colloids-Mery + 4.45 mgC/L HPO-SRNOM. Experimental conditions: Operational pressure =1.0 bar, temperature 20 ± 1°C, pH ~ 6 without PMS addition and 3.40 ± 0.10 with 1 mM PMS addition.

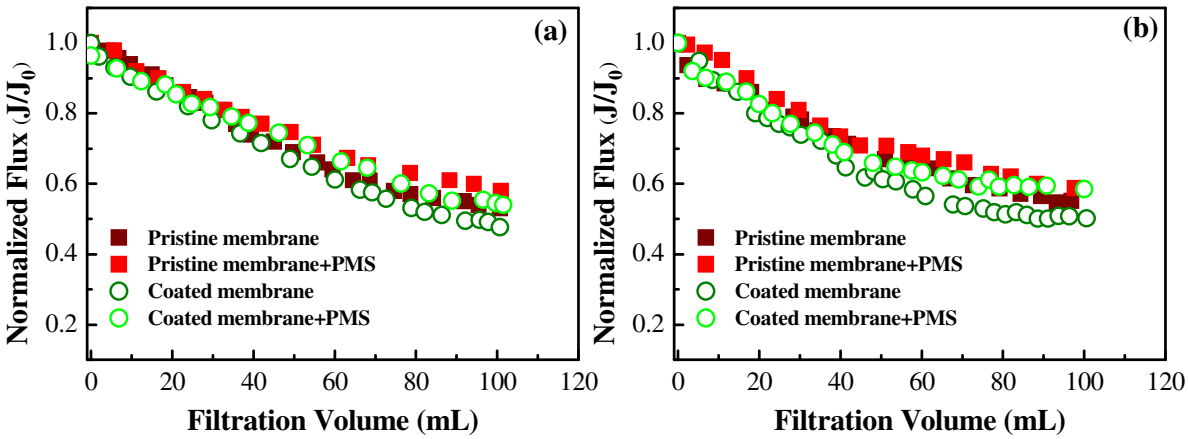

Fig. 4. Normalized water flux of the pristine and coated membrane with or without PMS addition in (a) NOM solution-B and (b) NOM solution-M. NOM solution-B: 0.56 mgC/L Colloids-Brittany + 4.45 mgC/L HPO-SRNOM, NOM solution-M: 0.55 mgC/L Colloids-Mery + 4.45 mgC/ L HPO-SRNOM. Experimental conditions: Operational pressure =1.0 bar, temperature 20 ± 1 °C, pH ~ 6 without PMS addition, and 3.40 ± 0.10 with 1 mM PMS addition.

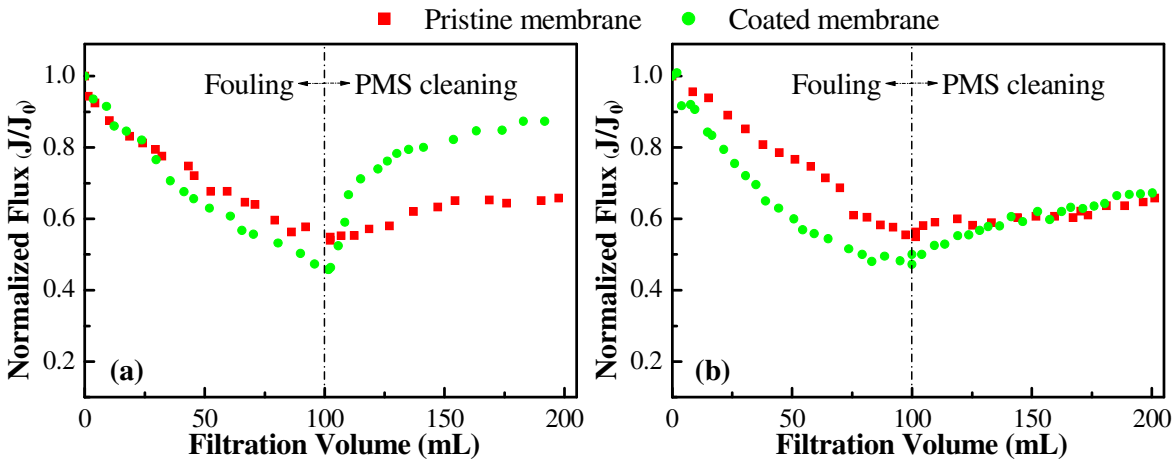

Fig. 5. Change in normalized water flux during fouling test and PMS cleaning for (a) NOM solution-B and (b) NOM solution-M fouled membrane. Conditions: Fouling tests were conducted with 100 mL of feedwater containing 0.56 mgC/L Colloids-Brittany + 4.45 mgC/L HPO-SRNOM for (a) and 0.55 mgC/L Colloids-Mery + 4.45 mgC/ L HPO-SRNOM for (b). Cleaning was performed with 100 mL of 10 mM PMS solution at pH 3.20 ± 0.10.

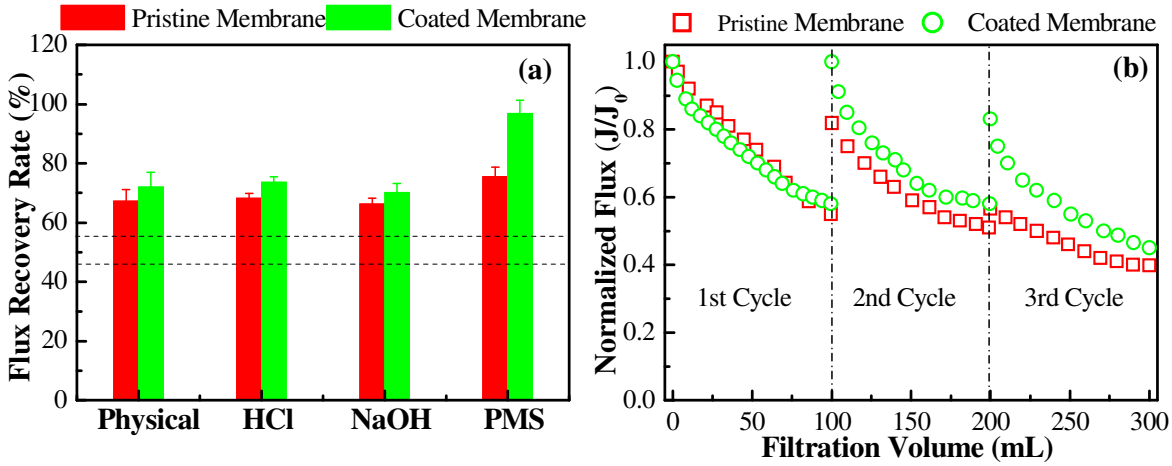

Fig. 6. Flux recovery rate with (a) multiple cleaning methods and (b) fouling profiles during filtration cycles with PMS cleaning applied between each fouling cycle for both pristine and coated membranes. Feedwater for fouling tests was prepared with a mixture of 0.55 mgC/L Colloids-Mery and 4.45 mgC/L HPO-SRNOM (pH 6.28). The black dash lines in Fig. 7a indicate the range of the values in normalized water flux before cleaning.

Table 1. R^2 values from the fitting of the experimental data with filtration models (R^2: coefficient of determination for different modelings; STDEV: Standard deviation in R^2 of duplicate modeling). The experimental data used for modeling was obtained from fouling tests using NOM solution-M.

	Complete Blocking		Intermediate Blocking		Standard Blocking		Cake Layer Filtration	
	R^2	STDEV	R^2	STDEV	R^2	STDEV	R^2	STDEV
Pristine	0.889	0.00	0.906	0.00	1.000	0.00	0.905	0.02
Pristine/PMS	0.792	0.00	0.771	0.04	0.999	0.00	0.812	0.01
Coated	0.876	0.03	0.872	0.03	1.000	0.00	0.879	0.05
Coated/PMS	0.862	0.06	0.882	0.05	1.000	0.00	0.889	0.03

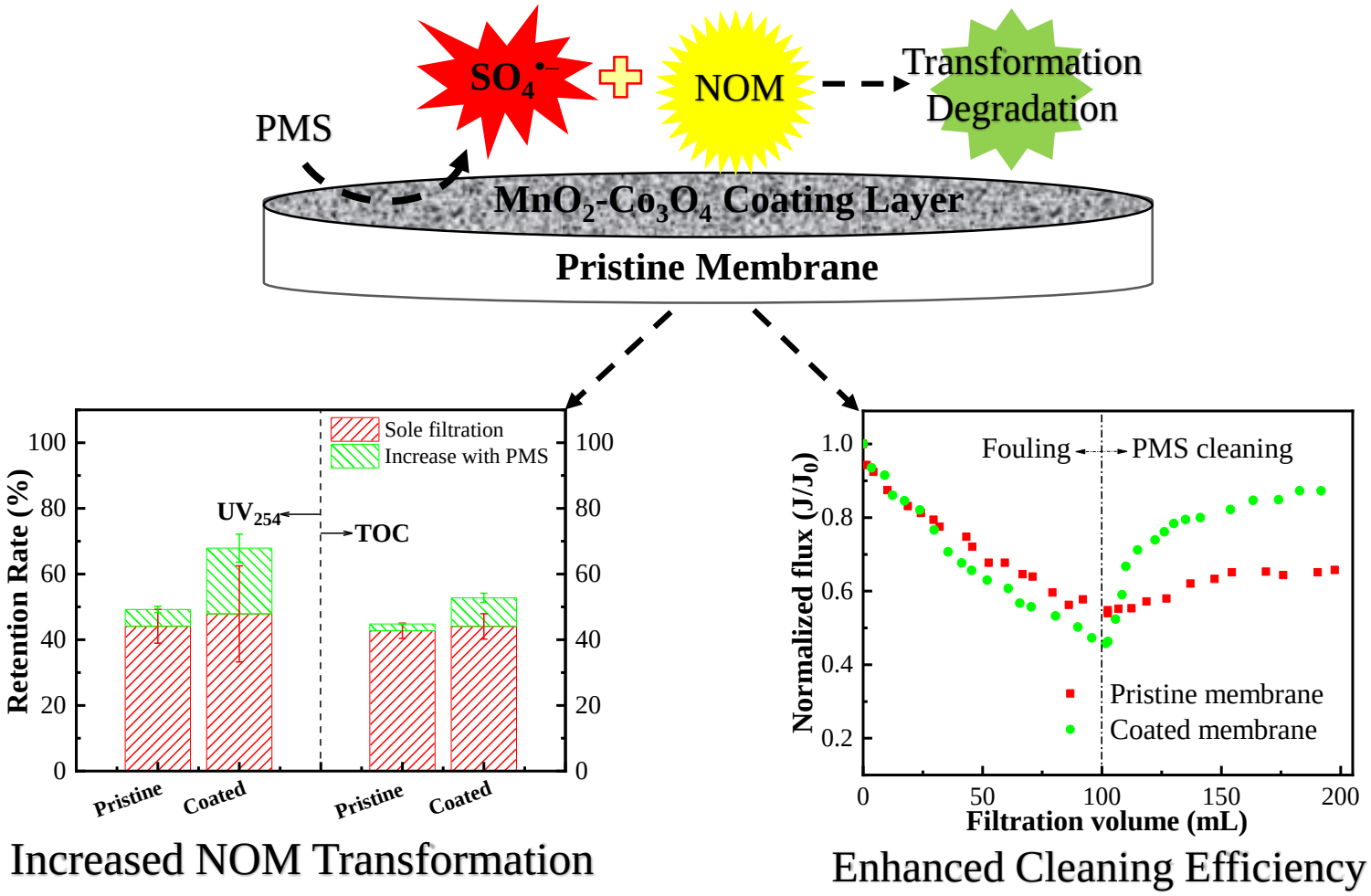

Increased NOM Transformation

Enhanced Cleaning Efficiency